NASA Technical Memorandum 81406

AN ANALYTICAL AND EXPERIMENTAL STUDY OF A SHORT S-SHAPED SUBSONIC DIFFUSER OF A SUPERSONIC INLET

Harvey E. Neumann, Louis A. Povinelli,
and Robert E. Coltrin
Lewis Research Center
Cleveland, Ohio

Prepared for the
Eighteenth Aerospace Sciences Meeting
sponsored by the American Institute of Aeronautics and Astronautics
Pasadena, California, January 14-16, 1980

AN ANALYTICAL AND EXPERIMENTAL STUDY OF A SHORT S-SHAPED SUBSONIC DIFFUSER OF A SUPERSONIC INLET

by Harvey E. Neumann,* Louis A. Povinelli,* and Robert E. Coltrin**
National Aeronautics and Space Administration
Lewis Research Center
Cleveland Ohio 44135

Abstract

An experimental investigation of a subscale HiMAT forebody and inlet was conducted over a range of Mach numbers to 1.4. The inlet exhibited a transitory separation within the diffuser but steady state data indicated reattachment at the diffuser exit. A finite difference procedure for turbulent compressible flow in axisymmetric ducts was used to successfully model the HiMAT duct flow. The analysis technique was further used to estimate the initiation of separation and delineate the steady and unsteady flow regimes in similar S-shaped ducts

Introduction

The inlet designer of advanced tactical aircraft must continually expand the stable flight and manuever envelopes. These advanced designs often lead to inlets which are characterized by short length, sharp curvatures, and large offsets. The associated requirements for high inlet performance and inlet/engine compatibility are becoming more difficult and close attention must be given to the quality of the flow at the diffuser exit.

The HiMAT is an example where vehicle design considerations have imposed severe geometric constraints on the inlet. In the HiMAT program, the test vehicle will demonstrate in flight the integrated effect of numerous new technologies. Although most major components of this RPRV were scaled from that of a man-sized high performance aircraft system, the inlet's geometric characteristics had to be compromised because of aircraft volume and engine considerations. The underbelly inlet is a fixed geometry, normal shock type with a three dimensional cross section. Compared with other similar configurations such as the F-16, this inlet has significantly shorter length, increased diffusion and sharper "s" wall curvatures.

When a subsonic diffuser is shortened, the nonuniformity of the flow at diffuser exit increases and duct separation or unsteady flow can exist. Four distinct flow regimes have been defined for two dimensional diffusers and have been related to the geometry of the configuration by Kline.[1] These characteristics are shown in Fig. 1. Although not defined in the literature, similar regimes exist for all other diffusers. Since short diffusers of the type used in advanced vehicles are prone to separate and produce high dynamic distortions at the compressor face, the HiMAT diffuser was studied both analytically and experimentally.

This paper will present results from the modeling of the HiMAT inlet using an axisymmetric viscous analysis and the subsequent experimental subscale HiMAT forebody/inlet distortion test in the NASA LeRC 8 by 6 Foot Supersonic Wind Tunnel. The modeling technique was further used to generalize the analytical results and delineate the steady and nonsteady flow regimes for similar S-shaped diffusers.

Apparatus and Procedure

Inlet Details

The RPRV HiMAT was designed for operation to Mach numbers in excess of 1.5. The test configuration was a 0.2884 scale model of the forebody and inlet and was tested to Mach 1.4 over a range of pitch and yaw angles and a range of engine airflows. Figure 2 shows the test model installed in the test section of the NASA Lewis 8 by 6 Foot Supersonic Wind Tunnel. The geometric shape of the HiMAT subsonic diffuser is shown in Fig. 3 and the axial distribution of area in Fig. 4. The relatively constant passage height in the initial portion of the diffuser is compensated by area changes in the sidewall region to provide a smooth area variation throughout the diffuser. The inlet was coupled to a coldpipe-choked plug assembly which maintained choked flow conditions a short distance downstream of the compressor face instrumentation (Fig. 5). The basic HiMAT inlet does not incorporate vortex generators, but a vortex generator study was conducted during the test. The specifications of the vortex generators used during the study are given in Fig. 6. Vortex generators were used on the ramp surface at an x/R_2 of 5.924 and on the cowl surface at an x/R_2 of 7.366. The size of the generators was based on computed flow conditions on the ramp surface at the upstream generator location. No adjustments in generator size were made for the side wall or for the downstream cowl surface flow conditions.

Instrumentation

The primary total pressure instrumentation is shown in the cutaway sketch (Fig. 5). Four boundary layer rakes were placed in the diffuser on the ramp surface to detect the predicted flow separation. The upstream rake was placed ahead of the anticipated separation whereas the other three rakes were used to define the separation region. The rakes were staggered circumferentially to avoid interference effects on downstream instrumentation. Forty combination steady state-dynamic total pressure probes were used at the compressor face to measure the diffuser exit conditions. These probes were arranged in a 5 ring by 8 rake probe configuration. The pressure probes were located at the center of equal areas. Only the fluctuating component of pres-

*Aerospace Engineer
**Head, Supersonic Propulsion Section

AIAA Paper No. 80-0386

sure was recorded from each dynamic probe. The fluctuating component of each pressure transducer was recorded on FM multiplexed tape. This component was later added to the corresponding time averaged (steady state) pressure during data analysis. The frequency response of the dynamic compressor face probes was flat to about 2000 Hz. All analysis of the dynamic data was performed on DYNADEC by AFFDL. The local static pressures were measured on both the ramp and cowl centerlines and by a row of side wall static taps.

Results and Discussion

The short length, high diffusion and sharp s-curvature of the HiMAT subsonic diffuser suggested a possibility of flow separation. To evaluate this possibility, the finite-difference procedure of Ref. 2, for turbulent compressible flow in axisymmetric ducts was used. This analysis procedure first obtains a potential flow solution which is used to establish a generalized orthogonal curvilinear coordinate network. The turbulent viscous effects are then retained in the formulation of the problem and the analysis is reinitiated to obtain a time marching solution with viscous effects included throughout. The program approximates the flow blockage and frictional effects of struts in the analysis.

To model the conformal inlet by an axisymmetric code, the geometry was simulated by a segment of an annular diffuser using the procedure of Ref. 3. The geometric simulation was constrained to preserve: (1) the HiMAT diffuser area ratio, (2) the HiMAT entrance height at the centerline, (3) the HiMAT exit height at the centerline (the compressor face diameter), and (4) the HiMAT offset on the ramp surface. These conditions also ensure that the offset on the cowl surface is maintained. The four constraints determine the exit and entrance radii for the inner and outer contours of the equivalent annular geometry. Struts were added of an appropriate number and thickness to provide the proper entrance area of HiMAT. The ramp and cowl contours of HiMAT at the centerline are then also preserved. The resultant geometric simulation is schematically shown in Fig. 7 and the comparison of the modeled and actual diffuser cross sections are compared in Fig. 8. This simulation does not accurately model the areas except at the diffuser entrance and exit and does not model secondary flows within the diffuser. The vehicle operating conditions chosen for the analysis were a free stream Mach number of 0.9, an altitude of 30 000 ft, a throat Mach number of 0.7 and zero angle-of-attack and yaw. An assumed boundary layer flow blockage of 0.9% was used. Figure 9 shows the resulting velocity ratio plot and Fig. 10 shows the resulting wall shear stress distributions. Kline in Ref. 1 has suggested that high subsonic inlet Mach numbers tend to promote early transitory unsteady flows in short conical diffusers. Since the entrance Mach number of this diffuser is also high subsonic and the analysis does not include secondary effects, the shear distribution on the ramp surface suggests a high probability that separation will occur at an x/R_{T1} of about 0.55. No conclusion can be drawn about the effects of this separation on the peak instantaneous distortion at the compressor face or whether reattachment will occur within the diffuser. The scale model of the HiMAT inlet, including the forebody and canards, was therefore built and tested in the Lewis 8x6 SWT to determine the separation characteristics and the associated effects on pressure recovery and distortion levels.

The axial distributions of static pressure on the ramp, cowl, and sidewall are given in Fig. 11. The distributions shown are for zero angle-of-attack and yaw and a free stream Mach number of 0.9. The pressure distributions show a strong expansion on the cowl and side surfaces near the diffuser entrance. A small expansion occurs on the ramp walls downstream to a x/R_c of about 8.4. This expansion is due to local boundary layer growth and wall curvature effects. The results of the analysis are also shown in the figure. The separation appears to take place near the sudden change in slope of the wall static pressure at $x/R_2 = 10.3$ shown in Fig. 11.

The flow along the ramp surface was surveyed at four axial locations. The total pressure distributions are shown in Fig. 12. The wall static pressures as obtained by interpolation from the ramp distribution of Fig. 11 are included on the profiles. The profile from the upstream rake is typical of a turbulent boundary layer and shows little free stream recovery loss. Each of the downstream rake profiles indicate high recovery loss and flow separation and an attendant loss in recovery. The initiation of the separation is therefore between an axial location of $x/R_c = 9.503$ and 10.939.

The steady state total pressure profiles at the compressor face are shown in Fig. 13. The recovery is plotted for each of the four quadrants. The local wall static pressure ratios are also shown. These data were measured with the mid diffuser rakes removed to eliminate any possible rake wake effect. Recovery on the cowl surface was generally very good except in the near wall region. The recovery profiles on the ramp surface clearly show a large reduction in pressure on the top centerline of the diffuser which was downstream of the flow separation. The near wall total pressures are higher than the measured wall static pressures. This indicates that flow reattachment has occurred. Examination of the dynamic pressure however indicates that transitory separation is present. A typical time history of the dynamic component of total pressure obtained from a typical dynamic pressure probe at the compressor face is shown in Fig. 14. The pressure trace shows a one-sided character. When the mean total pressure is assigned the steady state level of pressure as independently measured, the downward spiking extends from this mean steady state total pressure level down to the steady state static pressure level. This strongly suggests that at those instants of time when downward spiking occurs in the pressure traces, a transitory separation occurs at the compressor face. Additional creditability to this argument is obtained by noting that the upper level of the envelope of time varying pressures corresponds approximately to the mean free stream total pressure. The downward spiking in the pressure signals occurred randomly and was not associated with any particular frequency. The spiking were usually noted on the probes of the outer ring and on the probes downstream of the diffuser ramp separation. On occasion, however, they were

noted on each of the other dynamic pressure probes.

One well known technique for eliminating duct flow separation is the use of vortex generators. The vortex generators described previously were installed upstream of the separation zone to energize the low energy fluid near the wall. The effectiveness of the vortex generators was determined by using the downstream diffuser boundary layer rake. The total pressure profile is compared to the comparable profile without generators in Fig. 15. The profile shows that separation was eliminated by the vortex generators. Examination of the dynamic traces confirmed that the transitory separation also had been eliminated.

The average total pressure recovery measured at the compressor face is shown in Fig. 16. Results are presented for operation both with and without vortex generators. The data shown is for nominal vehicle operating conditions which are:

Mach number	Angle-of-attack, deg	Angle-of-yaw, deg
0.6	3.0	0
.9	7.0	0
1.2 & 1.4	4.0	0

The recovery which corresponds to the zero angle-of-attack data presented in Figs. 11 to 15 is shown by the filled symbol. The recoverys are very good over the entire range of operation despite the presence of the upstream separation on the diffuser surface and the compressor face transitory separation. The addition of the vortex generators reduced the recovery about 1 percent over the Mach number range.

The distortion in terms of ΔPRS, the distortion methodology for the J85-GE-21, is presented in Fig. 17. The distortion is the peak instantaneous distortion obtained from the analysis by AFFDL using DYNADEC. Each value of distortion was obtained from a 30 second recording of dynamic pressure data. The data was processed using a 500 Hz low pass filter to account for engine response. The recommended limit for the J85-GE-21 engine is also shown for operation at a 40 000 foot altitude. This limit assumes a normal engine operating with a unrestricted throttle. The distortion delivered by the inlet is lower than the engine limits for all operating conditions shown. The figure also shows the distortion when vortex generators were added. The peak distortion is significantly reduced when the vortex generators were installed except at the low Mach numbers. The generally higher distortion without the vortex generators is a result of a difference in the character of the distortion. The basic pressure patterns and hence the distortion changes when vortex generators are installed in the diffuser. Without generators, the peak distortion always occurs during that instant of time when transitory separation is present at the compressor face. The pressure distribution is characterized by a large "hole" downstream of the diffuser separation. This gives rise to large values for both the circumferential and radial distortion indices. The J85-GE-21 engine can however tolerate higher levels of circumferential distortion when accompanied by elevated levels of radial distortion. The resultant measured instantaneous distortion in terms of ΔPRS is modest. When generators are installed the large "hole" in pressure is no longer present. As a result the radial and the circumferential distortions are reduced to about half the previous values. The value of ΔPRS is not reduced by the same amount however since the reduction in radial distortion causes an increase in ΔPRS which is not offset by the reduced circumferential distortion.

The experimentally measured profiles of total pressure at the diffuser exit are compared to the predicted profiles in Fig. 18. In the modeling no engine hub was included. The experimental profiles that are presented are for the centerline rakes on the ramp (top) and cowl (bottom). The ramp side measured pressures do not agree with the predictions because of the effects of the separation. The agreement between the predicted and experimental pressure profiles on the cowl side of the diffuser is considered excellent.

The agreement shown between the static pressures (Fig. 11) and total pressures (Fig. 18) suggest that the modeling technique may be generalized to define or delineate the separation characteristics of similarly shaped diffusers. Kline in Ref. 1 showed that the flow regimes of conical diffusers and two dimensional diffusers correlate in terms of θ, the diffuser half angle and the nondimensional length. Specifically, the area ratio can be expressed as

$$A_2/A_1 = 1 + 2(\sin\theta)L/L_{ref}$$

For two dimensional diffusers the reference length used in the correlation was determined to be the inlet passage height and for conical diffusers it was the inlet radius. The results of Kline have been recast in the form presented in Fig. 19. The "line of first stall" and the "line of appreciable stall" as determined by Kline are shown. The area ratio presented is a measure of the diffusion whereas the mean wall angle is a measure of the flow turning. Kline's correlation in this form suggests that it can be used as the basis of defining the flow for HiMAT type diffusers.

The modeling procedure previously presented was used to analyize the HiMAT type diffusers. A matrix of configurations was generated by varying the area ratio (constraint no. 1) and the axial length while preserving the other HiMAT Geometric constraints. Struts for the axisymmetric diffuser segment analysis were selected to preserve the diffuser exit area. This matrix of geometries is considered to be HiMAT-similar-geometries since the ramp and cowl centerline contours are preserved. The axial length was varied by applying a scale factor to the axial coordinates. For a given area ratio, configurations with various lengths were then analyized until a diffuser separation was analytically encountered. The results of the analysis are presented in Fig. 19 in terms of the area ratio and the average wall angle of the surface on which separation was obtained with the wall shear stress as a parameter. The value of wall shear stress presented is the minimum value within the diffuser. The line of zero wall shear stress agrees very well with the line of appreciable stall. The second set of conditions are for a

wall shear coefficient of 0.0002. This value was obtained in the HiMAT analytical results of Fig. 10 and was shown experimentally to result in transitory separation. These results are in good agreement with Kline's line of first stall.

The agreement between the HiMAT class of diffusers and Kline's Stanford two dimensional diffuser correlation is considered adequate for defining flow regimes.

It should finally be noted that all of the results presented in this paper are for HiMAT ramp and cowl centerline contours and the applicability of the results to other configuration has not been determined.

Concluding Remarks

A wind tunnel investigation of the HiMAT forebody and inlet was conducted over a range of Mach numbers to 1.4. The experimental results were compared to analytical predictions from a finite difference procedure for turbulent compressible flow in axisymmetric ducts. The results indicate the following:

1. The average total pressure recovery at the compressor face was high over the nominal vehicle operating conditions. The peak instantaneous distortion obtained during operation at nominal conditions was less than the recommended limit for the J85-GE-21 engine.

2. Separation was noted for all operating conditions within the subsonic diffuser. Steady state total pressure profiles at the diffuser exit indicated reattached flow; however, dynamic pressure data indicated the presence of a transitory separation. The addition of vortex generators in the diffuser eliminated the duct separation.

3. The duct flow was analytically modeled as a segment of an axisymmetric annular diffuser. The shear stress results indicated a high risk of duct separation. The static pressure predictions on the walls of the diffuser and the total pressure distributions at the diffuser exit compared favorably with the experimental data in those portions of the flow field not affected by the flow separation.

4. The analysis technique was used to estimate the initiation of separation and delineate the steady and unsteady flow regimes in similar s-shaped ducts.

Symbols

A	area
d	distance from surface
h	vertical height
H	annular height at diffuser exit station (tip radius-hub radius)
L	length
L_{ref}	reference length
p	static pressure
P	total pressure
r	radial distance from diffuser exit centerline
R	radius
R_{T1}	full scale tip radius at inlet throat for annular diffuser analytical program (214.86 cm)
R_2	full scale compressor face radius (22.987 cm)
x	axial distance
y	vertical distance

Subscripts:

ℓ	local
ref	reference
T	tip or cowl for annular diffuser analytical program
H	hub or ramp for annular diffuser analytical program
0	free stream
1	diffuser entrance station
2	diffuser exit station

References

1. Kline, S. J., Abbott, D. E., and Fox, R. W., "Optimum Design of Straight-walled Diffuers," Journal of Basic Engineering, Vol. 81, Sept. 1959, pp. 321-328; discussion 329-331.

2. Anderson, O. L., "Finite-Difference Solution for Turbulent Swirling Compressible Flow in Axisymmetric Ducts with Struts," NASA CR-2365, 1974.

3. Povinelli, Louis A., "High-Performance-Technology," NASA CP-2092, May 1979, pp. 445-462.

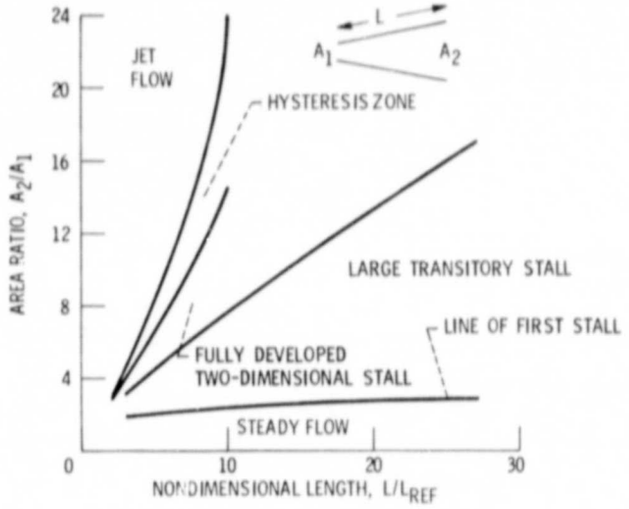

Figure 1. - Flow regimes for two-dimensional diffusers (ref. 1).

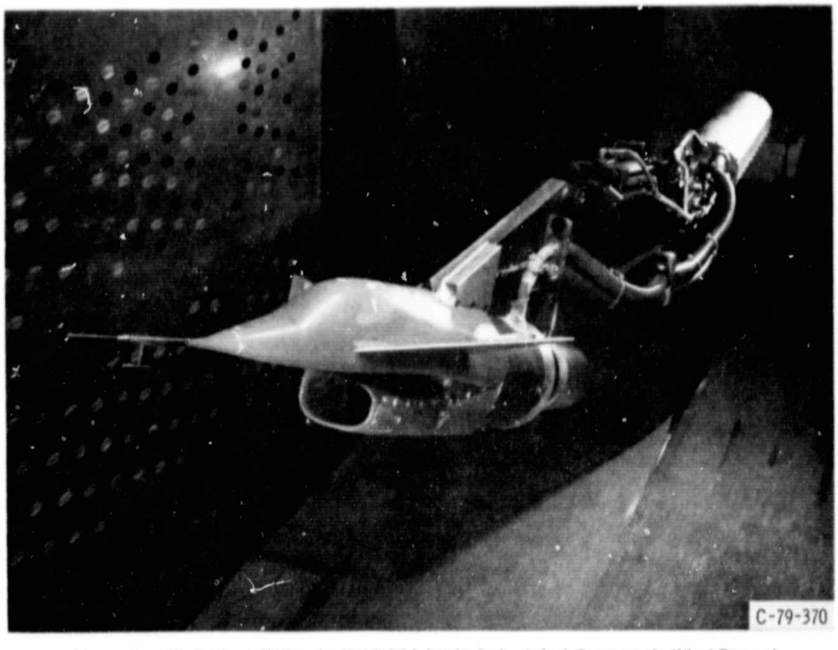

Figure 2. - Model installation in the NASA Lewis 8- by 6-foot Supersonic Wind Tunnel.

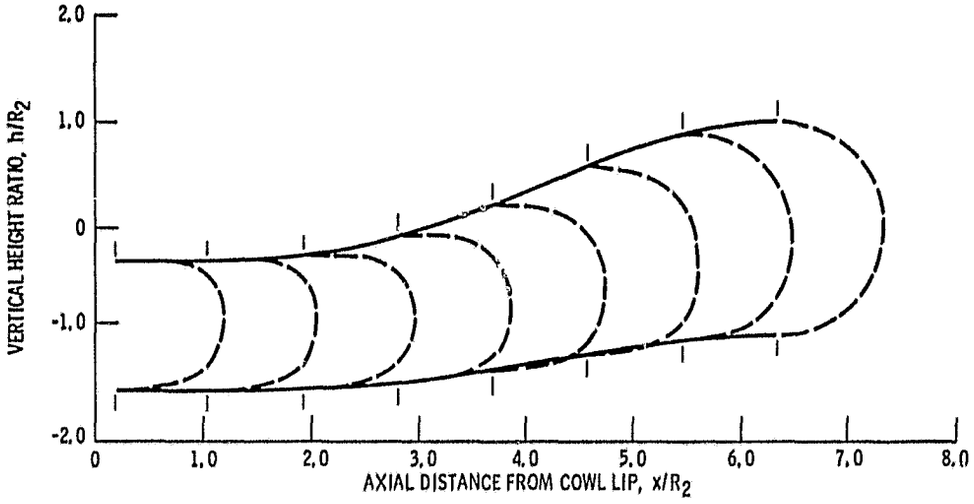

Figure 3. - Inlet internal contours.

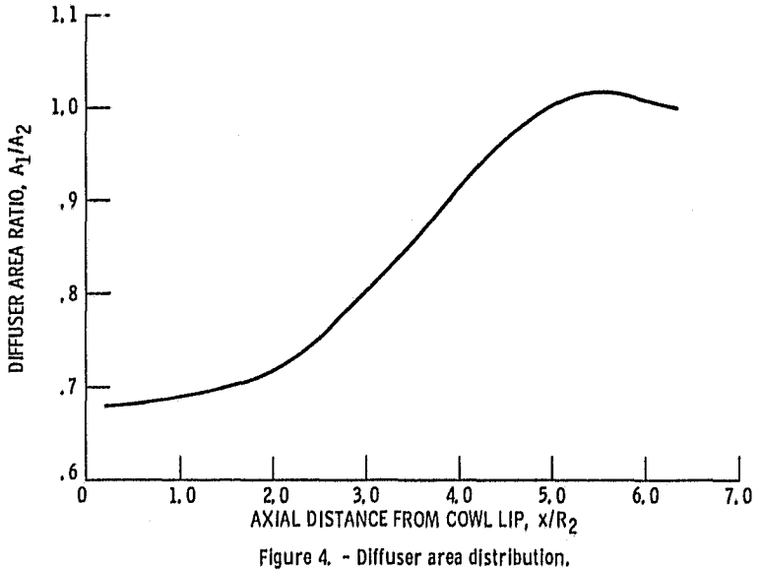

Figure 4. - Diffuser area distribution.

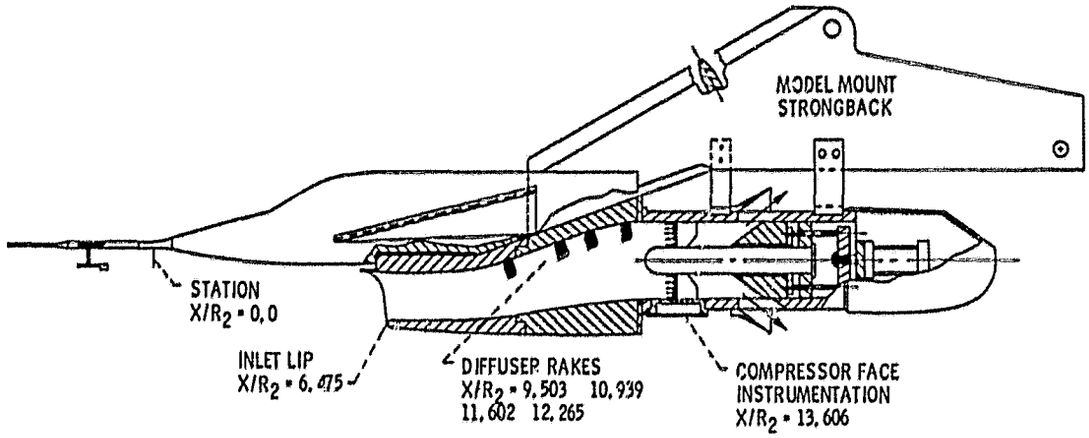

Figure 5. - Cutway illustrating inlet instrumentation and mass flow plug installation.

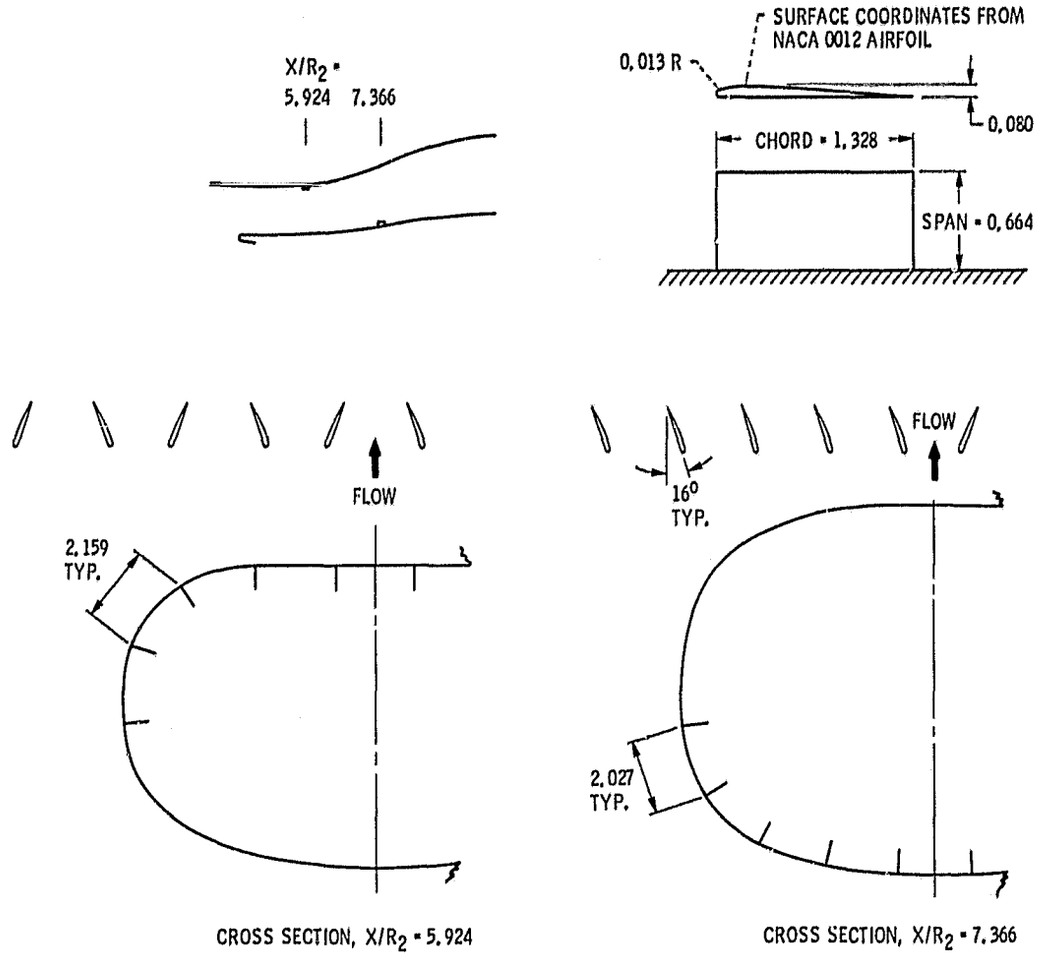

Figure 6. - Diffuser vortex generator details (dimensions in centimeters).

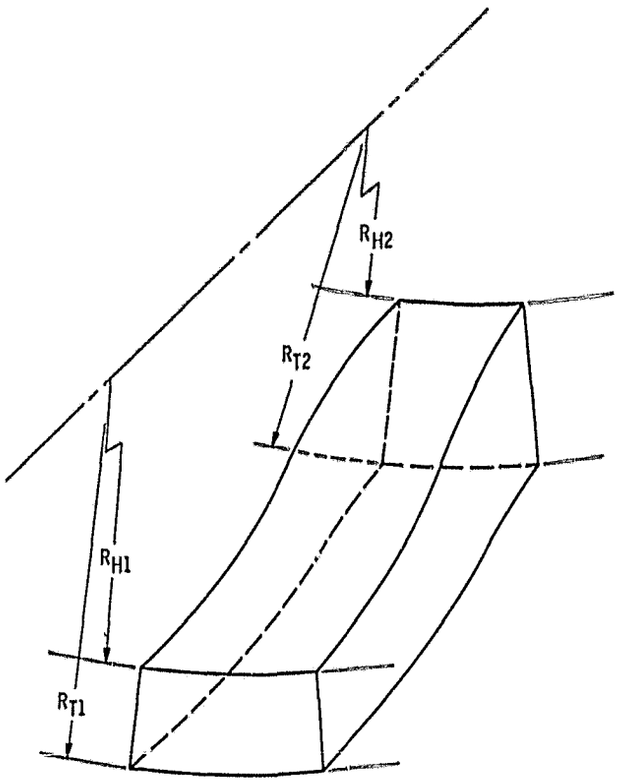

Figure 7. - Sketch of annular diffuser segment used in the analysis program to simulate the HIMAT diffuser.

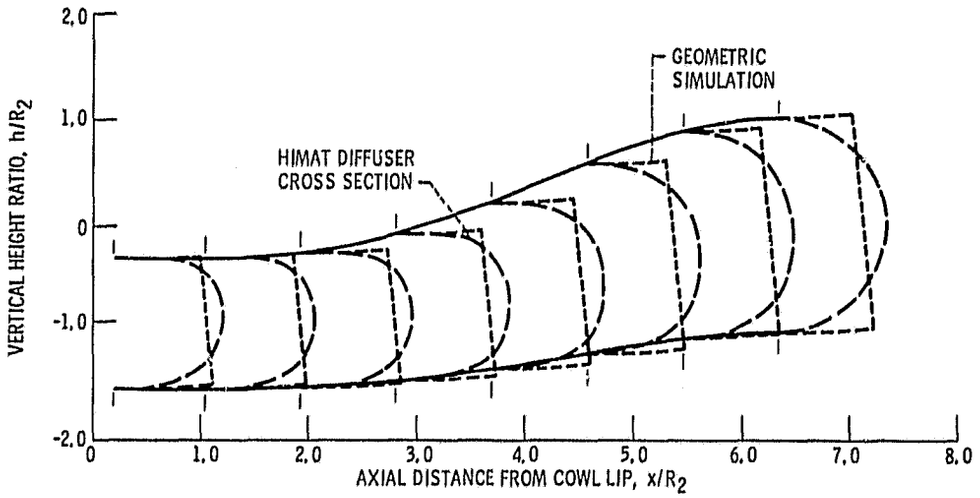

Figure 8. - Comparison of geometric simulation to actual diffuser cross sections.

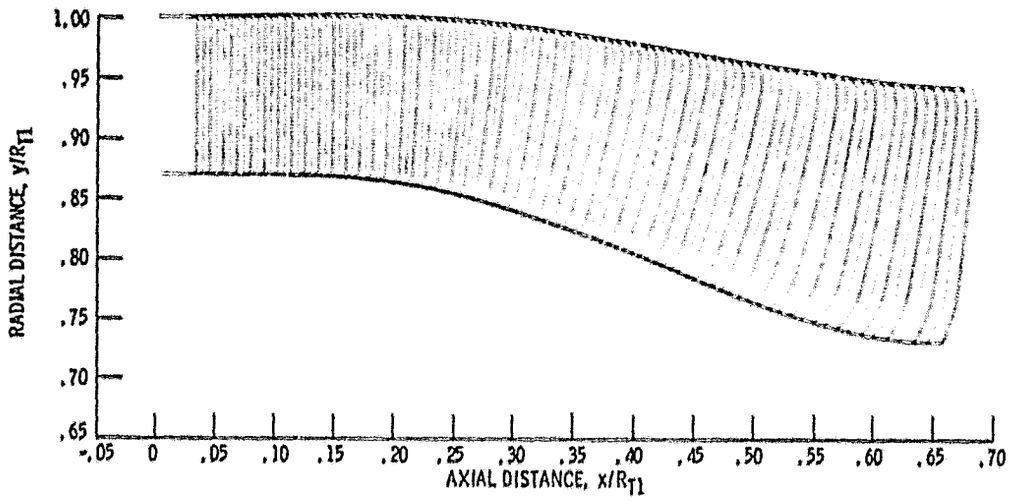

Figure 9. - Diffuser velocity distribution from analytical program.

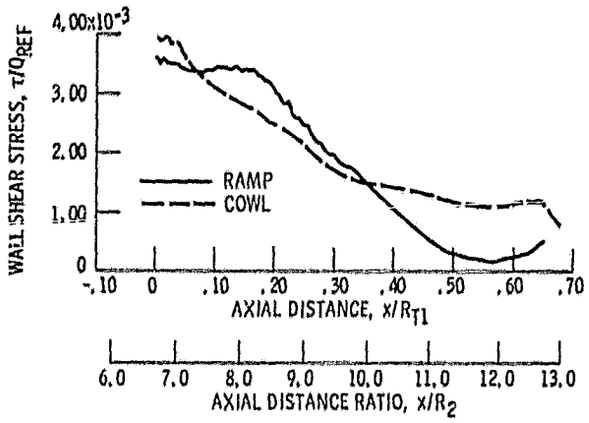

Figure 10. - Wall shear stress distribution.

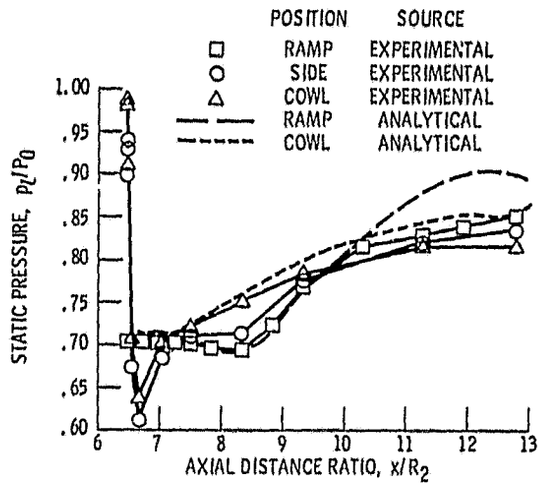

Figure 11. - Analytical and experimental distributions of wall static pressure.

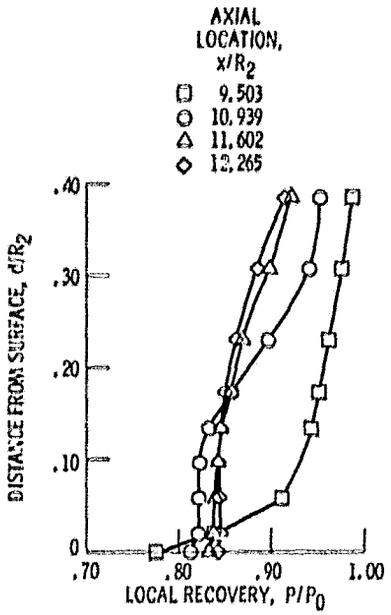

Figure 12. - Subsonic diffuser total pressure profiles.

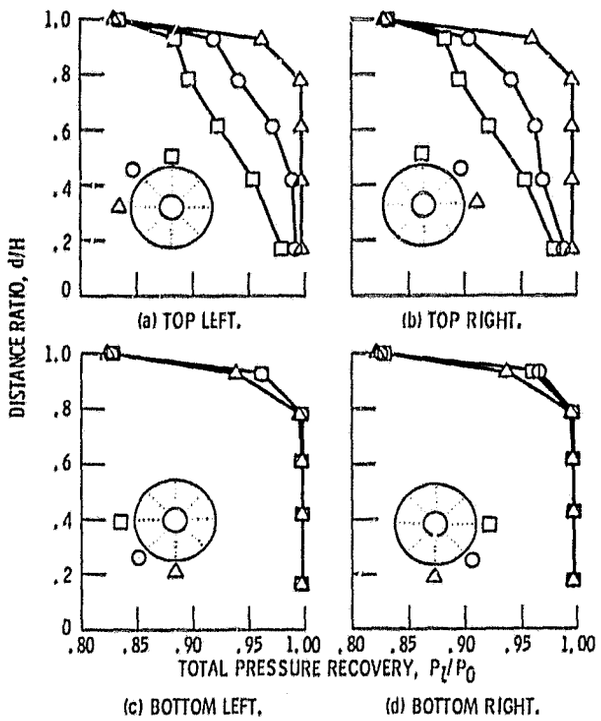

Figure 13. - Local distribution of compressor face recovery.

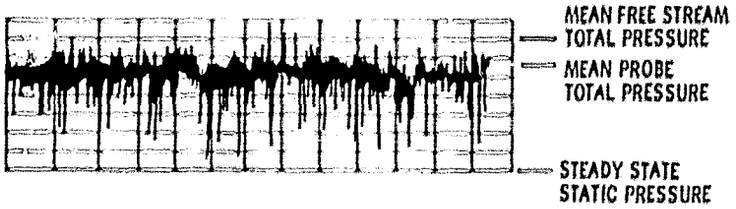

Figure 14. - Time history of typical compressor face total pressure.

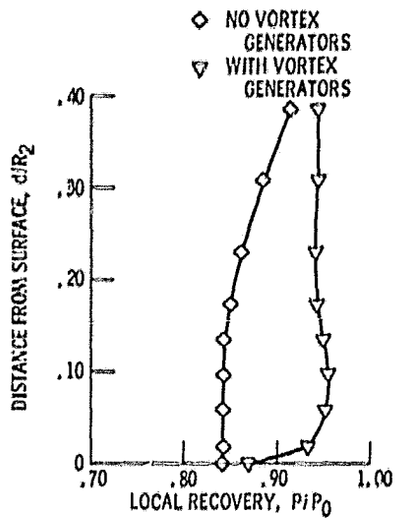

Figure 15. - Subsonic diffuser total pressure profile with and without vortex generators installed at diffuser station, x/R_2, 12.265.

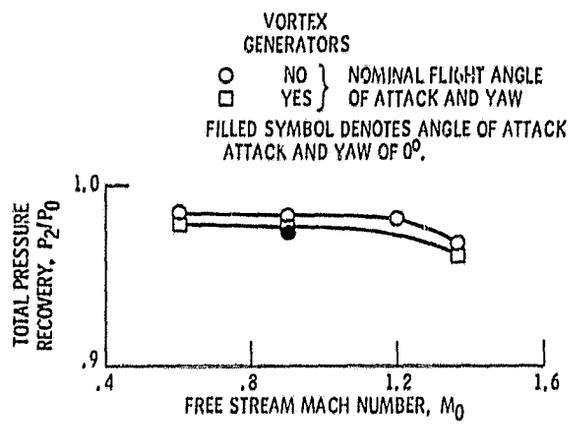

Figure 16. - Compressor face pressure recovery with and without vortex generators.

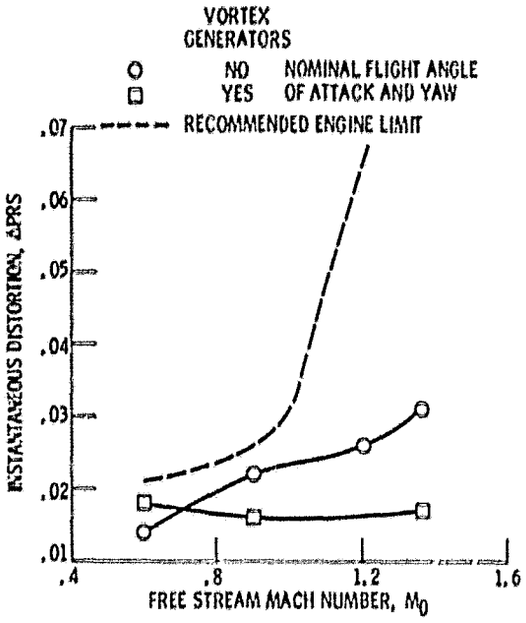

Figure 17. - Compressor face instantaneous distortion with and without vortex generators.

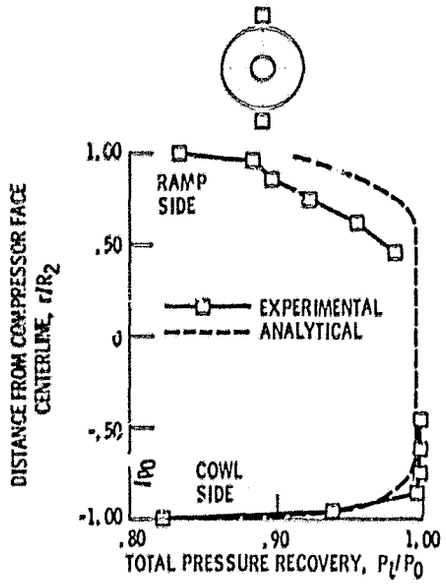

Figure 18. - Comparison of analytical and experimental compressor face total pressure profiles.

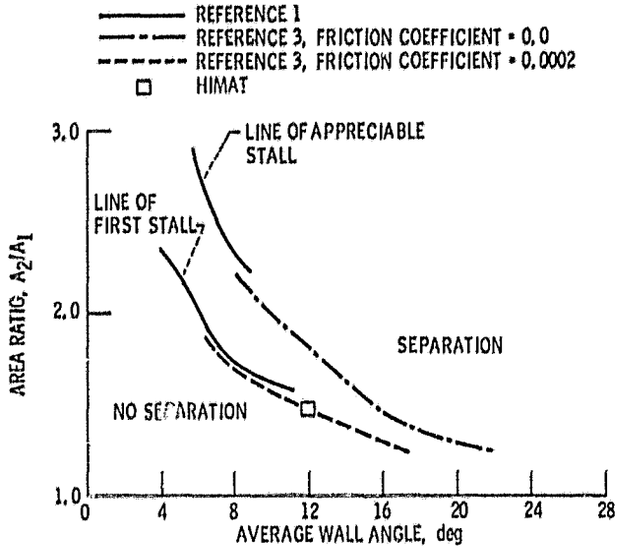

Figure 19. - Diffuser flow regimes.

1 Report No NASA TM-81406	2 Government Accession No	3 Recipient's Catalog No
4 Title and Subtitle AN ANALYTICAL AND EXPERIMENTAL STUDY OF A SHORT S-SHAPED SUBSONIC DIFFUSER OF A SUPERSONIC INLET		5 Report Date 6 Performing Organization Code
7 Author(s) Harvey E. Neumann, Louis A. Povinelli, and Robert E. Coltrin		8 Performing Organization Report No E-320 10 Work Unit No
9 Performing Organization Name and Address National Aeronautics and Space Administration Lewis Research Center Cleveland, Ohio 44135		11 Contract or Grant No 13 Type of Report and Period Covered Technical Memorandum
12 Sponsoring Agency Name and Address National Aeronautics and Space Administration Washington, D.C. 20546		14 Sponsoring Agency Code

15 Supplementary Notes

16 Abstract

An experimental investigation of a subscale HiMAT forebody and inlet was conducted over a range of Mach numbers to 1.4. The inlet exhibited a transitory separation within the diffuser but steady state data indicated reattachment at the diffuser exit. A finite difference procedure for turbulent compressible flow in axisymmetric ducts was used to successfully model the HiMAT duct flow. The analysis technique was further used to estimate the initiation of separation and delineate the steady and unsteady flow regimes in similar S-shaped ducts.

17 Key Words (Suggested by Author(s))	18 Distribution Statement
Diffusers Intakes Supersonic inlets Distortion	Unclassified - unlimited STAR Category 07

19 Security Classif. (of this report)	20 Security Classif. (of this page)	21 No. of Pages	22 Price*
Unclassified	Unclassified		

* For sale by the National Technical Information Service, Springfield, Virginia 22161